

16 † Niels Bohr Institute, University of Copenhagen, Universitetsparken 5, 2100 Copenhagen Ø,
17 Denmark

18 † Carl von Ossietzky Universität Oldenburg, School of Mathematics and Science Department of
19 Chemistry, 26111 Oldenburg, Germany

20 † Institute of Applied and Physical Chemistry, University of Bremen, Leobenerstraße, 28359
21 Bremen, Germany

22

23

24 **Corresponding Authors**

25 * E-mails: matthias.arenz@dcb.unibe.ch, jonathan.quinson@chem.ku.dk

26

27

28

29

30

31

32

33

34 **Table S1.** Examples from literature focusing on the surfactant-free polyol process.

Reference	Date	Platinum concentration / mM	NaOH concentration range / mM	Range of Base/Pt molar ratio	Different Platinum concentrations studied
1	2000	0.37-51	The pH was adjusted to 12, probably involuntarily keeping the NaOH/Pt ratio constant		YES
2	2006	28	200 -100	7.1 - 3.6	NO
3	2012	5.4	453 - 10	84 - 2	NO
4	2015	10	500 - 62.5	50 - 6.25	NO
5	2016	6	42 - 12	7 - 2	NO
6	2017	2	250 - 0	125 - 0	NO

35 Different metal complexes, different synthesis parameters (volume, time synthesis, mode of
 36 synthesis, etc.) were used. The summary focused on colloidal synthesis of monometallic
 37 platinum nanoparticles and excludes one-pot synthesis directly on a support except for [5].

38

39

40

41

42

43

44

45

46

47 **Table S2.** Experimental synthesis conditions for the data presented in Figure 2 and the
48 size estimated from SAXS measurements.

Volume / mL	Platinum concentration / mM	NaOH concentration / mM	NaOH/Pt molar ratio	Diameter (nm)
4	10	250	25	1.10 ± 0.23
4	10	125	12.5	1.37 ± 0.32
4	10	109	6.3	2.52 ± 0.29
4	10	63	3.1	5.07 ± 0.18
4	5	125	25	1.05 ± 0.27
4	2.5	63	25	0.97 ± 0.34
4	1.25	31	25	1.09 ± 0.27

49

50 SAXS Analysis

51 Small-angle X-ray scattering (SAXS) was performed at the Niels Bohr Institute SAXSLab
52 instrument at University of Copenhagen. This instrument is equipped with a 100XL + micro-
53 focus sealed X-ray tube from Rigaku producing a photon beam with a wavelength of 1.54 Å. The
54 scattering patterns were recorded with a 2D 300 K Pilatus detector from Dectris. The two-
55 dimensional scattering data were azimuthally averaged, normalized by the incident radiation
56 intensity, the sample exposure time and the transmission and corrected for background and
57 detector inhomogeneities using standard reduction software. The background measurement was
58 on a pure ethylene glycol sample. The radially averaged intensity $I(q)$ is given as a function of
59 the scattering vector $q = 4\pi \cdot \sin(\theta) / \lambda$, where λ is the wavelength and 2θ is the scattering angle.

60 The background corrected scattering data was fitted with a model of polydisperse spheres
61 described by a volume-weighted log-normal distribution. The model expression for the intensity
62 is:

63 (1)
$$I(q) = C \int P_s^2(q, R) V(R) D(R) dR$$

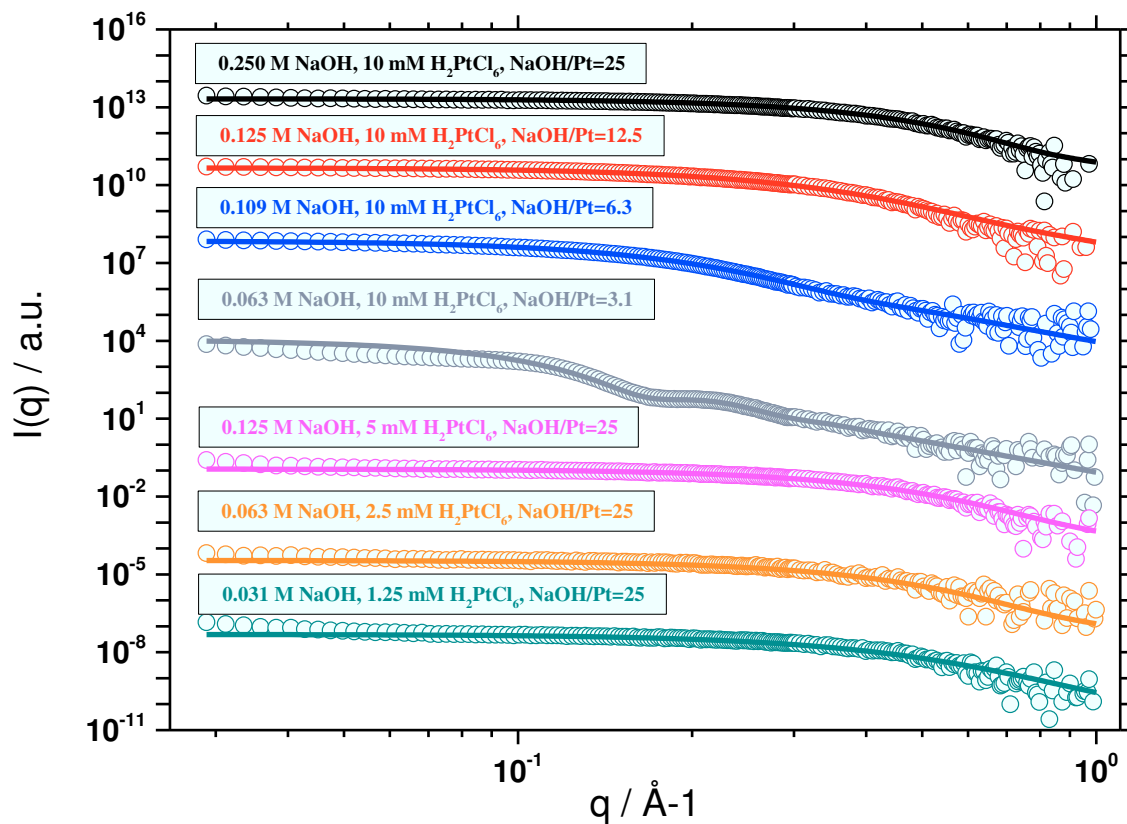
64 where C is an overall scaling constant, P_s is the sphere form factor, V the particle volume and D
65 the log-normal size distribution. The sphere form factor is given by:

66 (2)
$$P_s(q, R) = 4\pi R^3 \frac{\sin(qR) - qR \cos(qR)}{(qR)^3}$$

67 and the log-normal distribution by:

68 (3)
$$D(R) = \frac{1}{R\sigma\sqrt{2\pi}} \exp\left(-\frac{[\ln(\frac{R}{R_0})]^2}{2\sigma^2}\right)$$

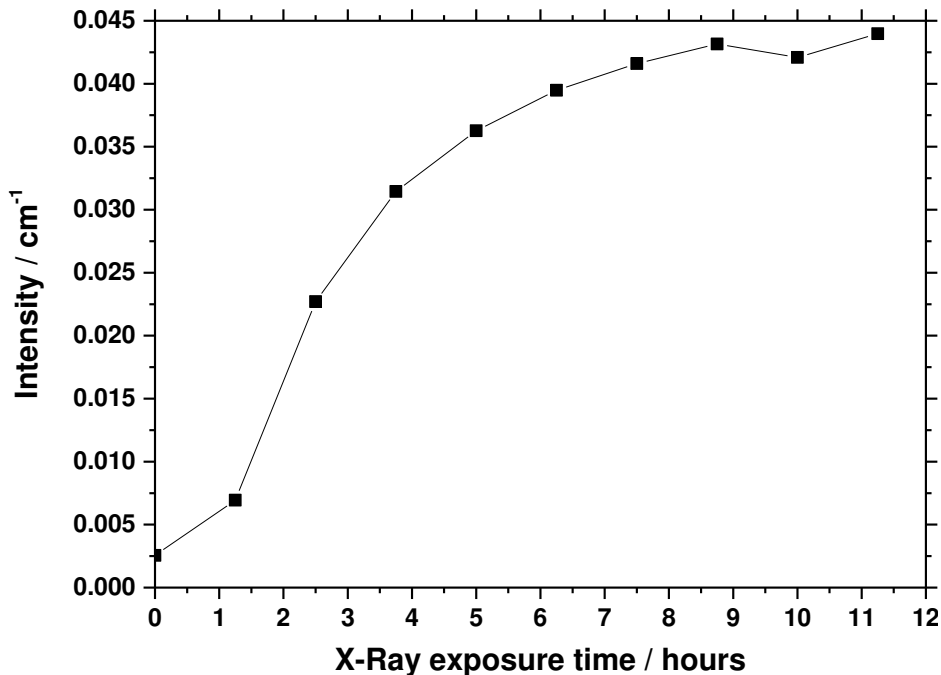
69 In one case it was necessary to include a structure factor contribution to model the data properly.
70 We employed a hard-sphere structure factor as described in Reference [7]. Basically, this
71 depends on the sphere radius and the sphere volume fraction. The fitting was done using home
72 written MATLAB code invoking a least-squares χ^2 -minimisation to optimise agreement between
73 data and model. Thus, the free parameters in the model are the radius and variance of the
74 polydisperse size distribution as reported in the paper. The scattering data and corresponding fits
75 can be seen in **Figure S1**.



76

77 **Figure S1.** SAXS data (circles) and corresponding fits (plain line) related to **Figure 2** in

78 the manuscript.



79
 80 **Figure S2.** Time evolution of SAXS intensity for $q = 0.086 \text{ \AA}^{-1}$ indicating that the X-ray beam
 81 induces particle growth (2 mM H_2PtCl_6 and 250 mM NaOH).

82
 83

84 **Hypothesis for the size control by the NaOH/Pt molar ratio**

85 A model to explain why the NaOH/Pt ratio controls the size is proposed. The hypothesis is that
 86 the nanoparticles will grow until a certain OH^- surface coverage is reached. As a result, the ratio
 87 between NaOH concentration and Pt surface atoms should be constant. This hypothesis is tested
 88 below by a rough estimation of the ratio of OH^- ions to Pt surface atoms (here called Ω) based on
 89 the obtained size of the nanoparticles (NPs) determined from the SAXS and TEM data:

90

$$\frac{\#(\text{OH})}{\#(\text{Pt surface atoms})} = \Omega \quad \text{eq. (1)}$$

91 Where # corresponds to the ‘number of’ and Ω is the ratio of OH to Pt surface atoms.

92 The total number of Pt atoms in a NP is estimated by:

$$93 \quad \# (Pt \text{ atoms per NP}) = 0.75 \frac{V (Pt NP)}{V (Pt atom)} \quad \text{eq. (2)}$$

94 Where V corresponds to ‘volume of’.

95 The total number of Pt surface atoms of a NP is given by:

$$96 \quad \# (Pt \text{ surface atoms per NP}) = 0.785 \frac{A (Pt NP)}{A (Pt atom)} \quad \text{eq. (3)}$$

97 Where A corresponds to ‘external surface area of’.

98 Experimentally given are the molar ratio between NaOH and Pt as well as the obtained NP size.

99 Assuming that $\#(NaOH \text{ per NP}) \sim \#(OH \text{ per NP})$, the molar ratio between NaOH and Pt is:

$$100 \quad \frac{NaOH}{Pt} \sim \frac{\#(NaOH \text{ per NP}) * \# (NPs)}{\# (Pt \text{ atoms per NP}) * \# (NPs)} \sim \frac{\#(OH \text{ per NP})}{\#(Pt \text{ atoms per NP})} \quad \text{eq. (4)}$$

101 Inserting eq.1 into eq.4, we obtain:

$$102 \quad \frac{NaOH}{Pt} \sim \frac{\Omega * \# (Pt \text{ surface atoms per NP})}{\# (Pt \text{ atoms per NP})} \quad \text{eq. (5)}$$

103 And with eq.2 and eq.3:

$$104 \quad \frac{NaOH}{Pt} \sim \Omega * \frac{A (Pt NP)}{V (Pt NP)} * \frac{V (Pt atom)}{A (Pt atom)} * \frac{0.785}{0.75} \sim \Omega * \frac{Pt \text{ atom diameter}}{NP \text{ diameter}} \quad \text{eq. (6)}$$

105 Where the Pt atom diameter corresponds to the covalent diameter of a Pt atom taken as 0.27 nm.

$$106 \quad \Omega \sim \frac{NaOH}{Pt} * \frac{NP \text{ diameter}}{Pt \text{ atom diameter}} \quad \text{eq. (7)}$$

107 Under our hypothesis, Ω should be a constant.

108 Using the experimental results to estimate Ω we obtain the following values:

NaOH/Pt	NP diameter (nm)	# atoms in a NP	# atoms at the surface of a NP	% or surface atoms	Ω
25	1.1	52	53*	100*	104*
13	1.4	95	20	84	63
10	2.1	341	187	55	78
6	2.5	581	67	46	59
5.5	2.9	897	357	40	59
5	4.0	2353	679	29	74
4.5	5.5	6118	1284	21	92

109 *naturally the model needs to break down at extremely small particles

110 Despite using a very simplistic model, the value of Ω is rather constant and thus supports the
 111 hypothesis that the OH⁻ surface concentration is not only responsible for the stabilization of the
 112 particles, but also the stop of the growth process.

113

114 **Table S3.** Properties of Pt nanoparticles obtained with different NaOH/Pt ratio from different
 115 characterization methods.

Characterization		NaOH/Pt	
		10	4.5
TEM	Diameter / nm	2.0 ± 0.6	3.6 ± 0.8
			5.5 ± 1.6
FTIR	CO peak / cm ⁻¹	2020	2045
XAS (EXAFS)	N(Pt-Pt ₁)	6.6 ± 0.7	8.7 ± 1.4
	R(Pt-Pt ₁) / Å	2.755 ± 0.005	2.758 ± 0.008
	R _f	0.015	0.013

	$\Delta E_0 / \text{eV}$	4.8 ± 0.7	$6.4 \pm 1.4 \text{ eV}$
	$\sigma^2 \times 10^{-4} / \text{\AA}^2$	56 ± 5	57 ± 6
PDF	$R_w / \%$	16.3	15.1
	Unit cell / \AA	3.930	3.941
	$B_{\text{iso}} / \text{\AA}^{-2}$	1.03	0.92
	$\text{delta}2 / \text{\AA}$	3.98	3.75
	Crystallite size / nm	2.2	3.8

116 *Diameter analysis:* when the NaOH/Pt molar ratio decreases the reproducibility of the size
117 control decreases, the two values quoted for NaOH/Pt of 4.5 are the extreme values obtained for
118 different samples prepared. It can be concluded that the NaOH/Pt ratio of 4.5 lead to
119 nanoparticles in the size range 3-5 nm. In contrast good reproducibility is obtained for NaOH/Pt
120 molar ratio of 10.

121 *XAS analysis:* N is the coordination number (indicative of the average number of neighboring
122 atoms). R is the interatomic bond length. R_f indicates the closeness of the fit to the data as
123 quality parameter. σ^2 is the mean squared bond length disorder. ΔE_0 is the correction to the
124 energy origin.

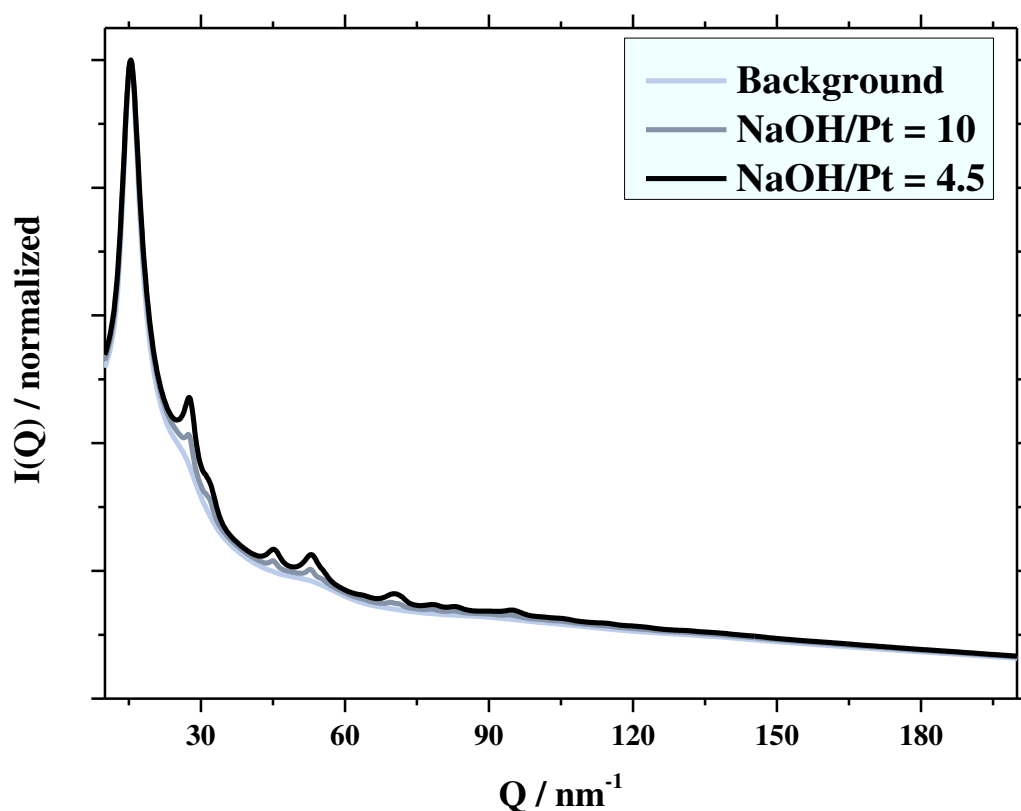
125 *PDF analysis:* R_w is a measure of the fit quality (lower value corresponds to better fit). B_{iso}
126 describes atomic motion of the Pt nanoparticles. $\text{delta}2$ relates to correlated motion between
127 neighboring atoms.

128

129 XAS. From X-ray absorption near edge structure XANES data (not shown), it is confirmed that
130 while the initial precursor consists in the form of Pt(IV), after synthesis mainly Pt(0) can be
131 detected. From EXAFS data, no fit could be obtained for the nanoparticles after synthesis that
132 could be assigned to Pt-Cl. These results suggest the total consumption of the initial H_2PtCl_6
133 precursor.

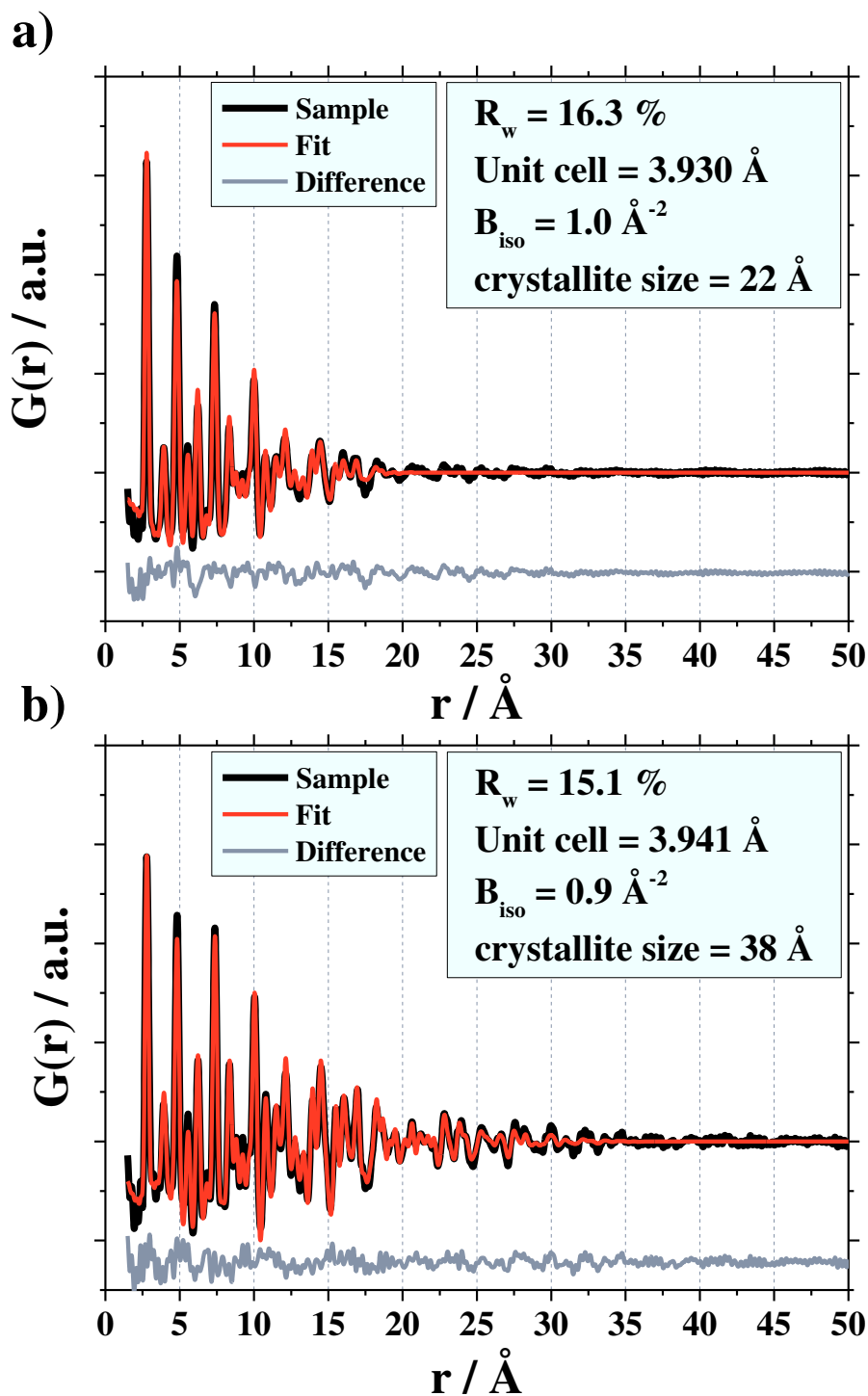
134 *PDF*. The unit cell parameter decreases with decreasing size, as expected for Pt nanoparticles.⁸
135 The B_{iso} values increase with size, which may account for structural disorder possible arising
136 from bond softening and disorder.⁹

137



138
139 **Figure S3.** Normalized intensity of X-ray total scattering for PDF analysis of Pt
140 nanoparticle obtained with different NaOH/Pt molar ratio as indicated.

141

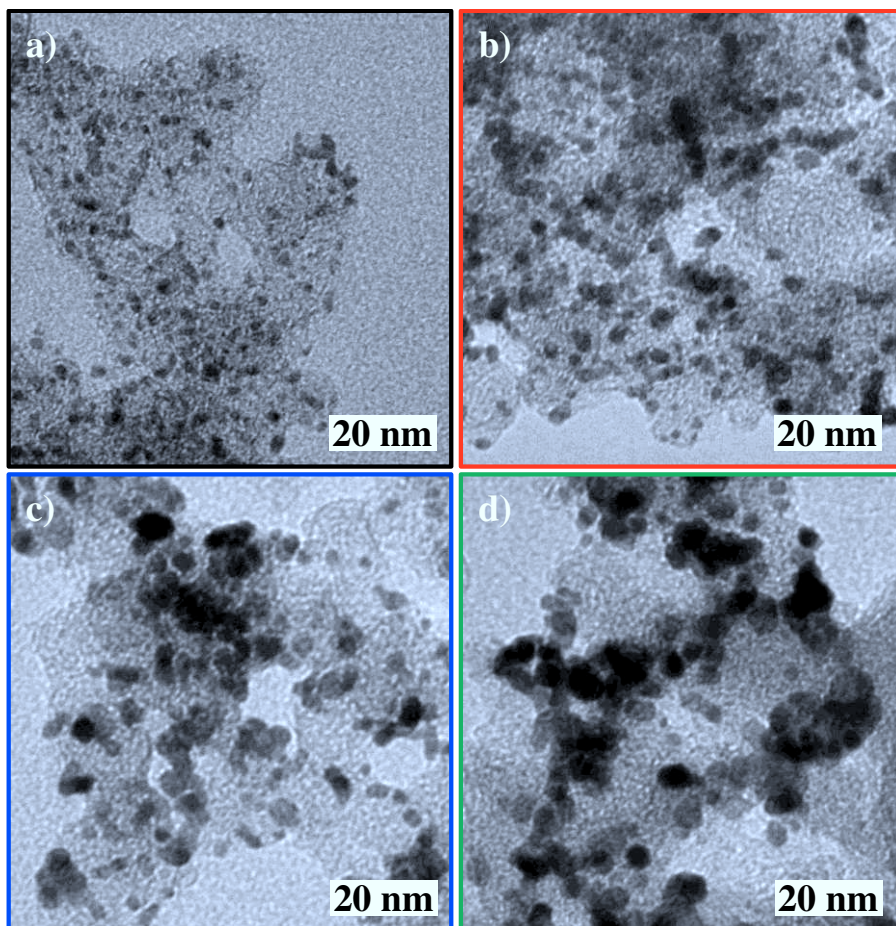


142

143 **Figure S4.** PDF characterization of the obtained Pt nanoparticles prepared with a

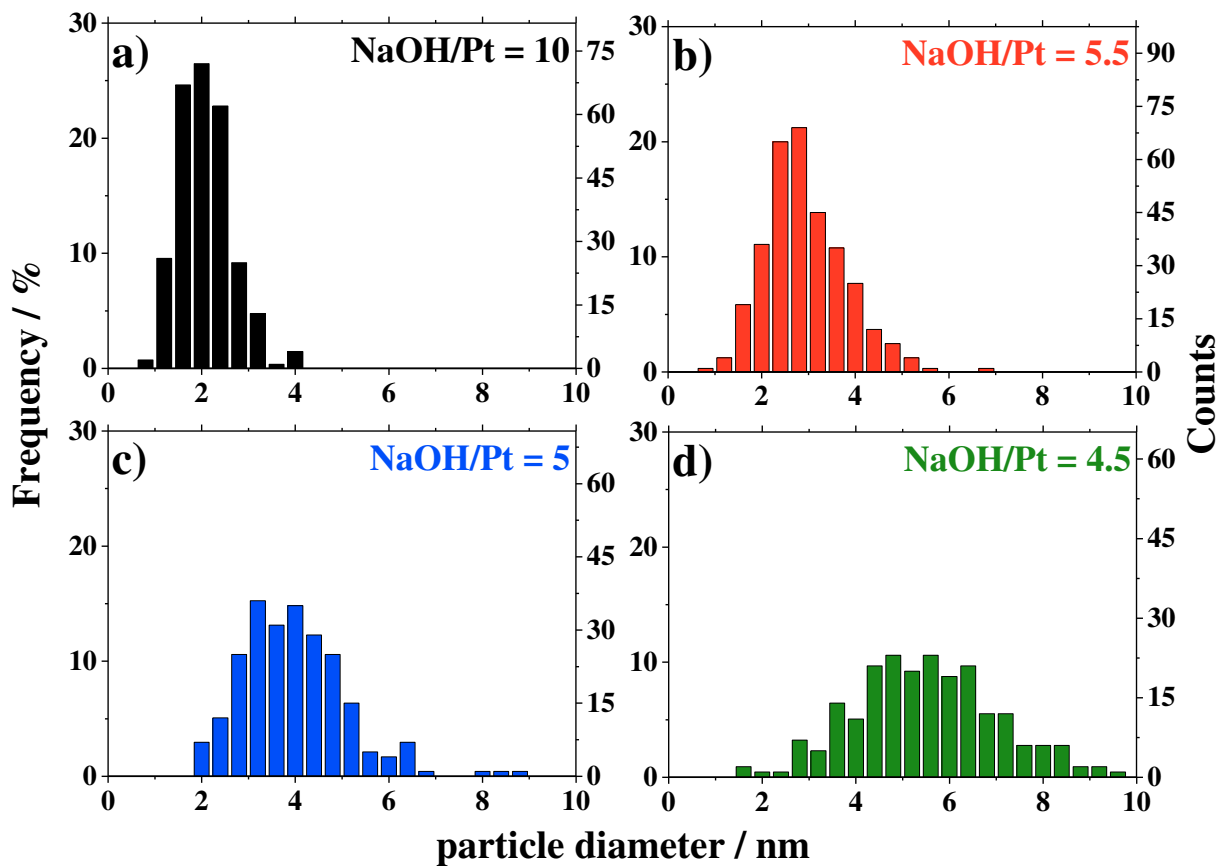
144 NaOH/Pt molar ratio of (a) 10 and (b) 4.5.

145



146
147 **Figure S5.** TEM micrographs of catalysts with a nominal 50 wt. % Pt on carbon (Vulcan
148 XC72R) obtained using nanoparticles synthesized using NaOH/Pt molar ratio of: (a) 10, (b) 5.5,
149 (c) 5 and (d) 4.5.

150
151
152
153
154
155
156



157

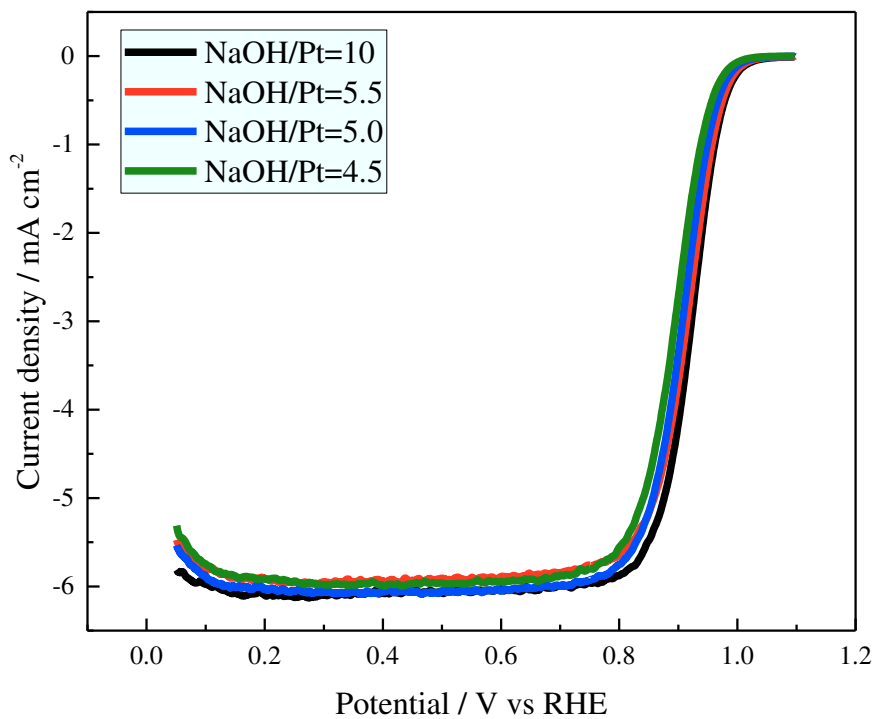
158 **Figure S6.** Particle size distribution estimated from TEM micrographs for Pt
 159 nanoparticles prepared with different NaOH/Pt molar ratio as indicated: (a) 10, (b) 5.5, (c)
 160 5 and (d) 4.5.

161

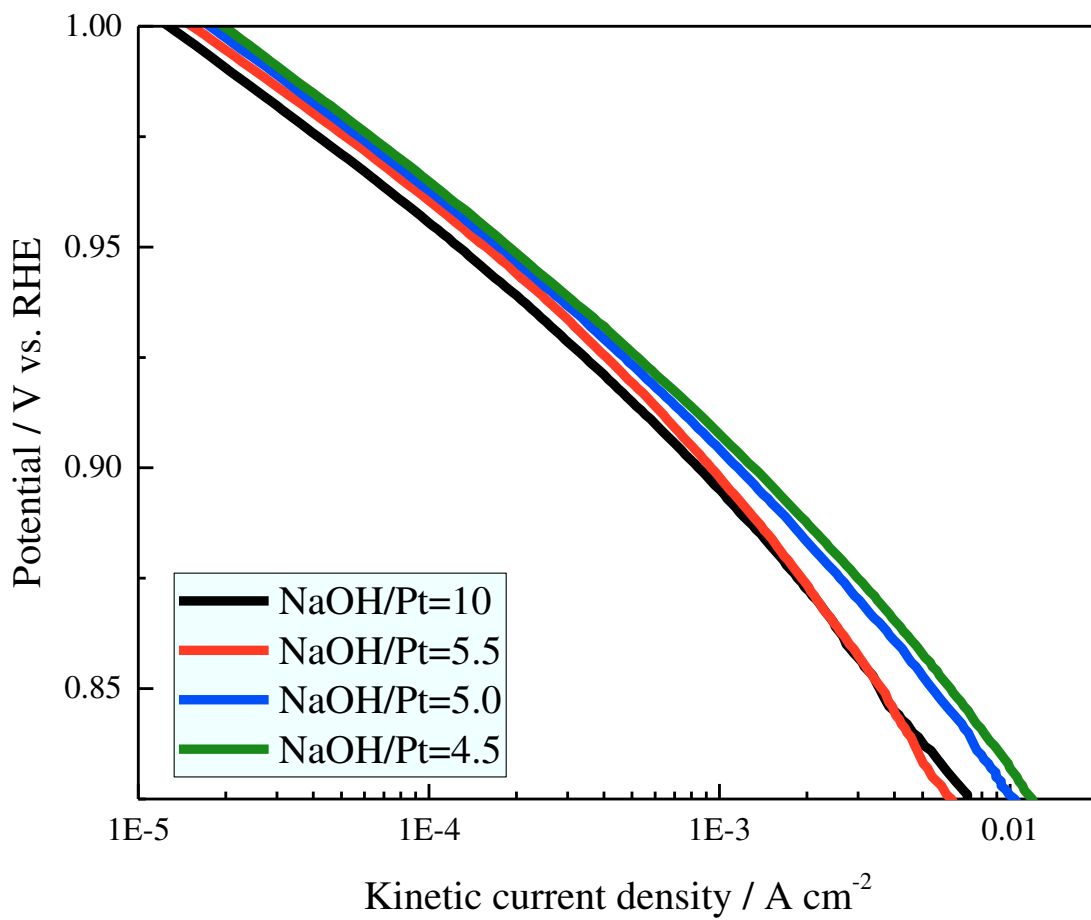
162

163

164



165
 166 **Figure S7.** Linear sweep voltammograms (positive scans) for Pt/C catalysts prepared from
 167 different colloidal Pt particle suspensions. The nominal Pt loading on the high surface area
 168 carbon support and the glassy were kept constant at 50 wt. % and $14 \mu\text{g}_{(\text{Pt})} \text{cm}^{-2}$, respectively.
 169 The measurements were conducted in O_2 -saturated 0.1 M HClO_4 at scan rate of 50 mV s^{-1} with
 170 1600 rpm.



171
172 **Figure S8.** Tafel plots obtained by extrapolating the linear sweep voltammograms in Figure S3
173 with the Koutecky-Levich equation.

174
175
176
177
178
179
180
181

- 183 1. Wang, Y.; Ren, J. W.; Deng, K.; Gui, L. L.; Tang, Y. Q., Preparation of tractable
184 platinum, rhodium, and ruthenium nanoclusters with small particle size in organic media.
185 *Chemistry of Materials* **2000**, *12* (6), 1622-1627.
- 186 2. Baranova, E. A.; Bock, C.; Ilin, D.; Wang, D.; MacDougall, B., Infrared spectroscopy on
187 size-controlled synthesized Pt-based nano-catalysts. *Surface Science* **2006**, *600* (17), 3502-3511.
- 188 3. Steinfeldt, N., In Situ Monitoring of Pt Nanoparticle Formation in Ethylene Glycol
189 Solution by SAXS-Influence of the NaOH to Pt Ratio. *Langmuir* **2012**, *28* (36), 13072-13079.
- 190 4. Schrader, I.; Warneke, J.; Neumann, S.; Grotheer, S.; Swane, A. A.; Kirkensgaard, J. J.
191 K.; Arenz, M.; Kunz, S., Surface Chemistry of "Unprotected" Nanoparticles: A Spectroscopic
192 Investigation on Colloidal Particles. *Journal of Physical Chemistry C* **2015**, *119* (31), 17655-
193 17661.
- 194 5. Aoun, N.; Schlange, A.; dos Santos, A. R.; Kunz, U.; Turek, T., Effect of the OH-/Pt
195 Ratio During Polyol Synthesis on Metal Loading and Particle Size in DMFC Catalysts.
196 *Electrocatalysis* **2016**, *7* (1), 13-21.
- 197 6. Kacenauskaite, L.; Quinson, J.; Schultz, H.; Kirkensgaard, J. J. K.; Kunz, S.; Vosch, T.;
198 Arenz, M., UV-Induced Synthesis and Stabilization of Surfactant-Free Colloidal Pt
199 Nanoparticles with Controlled Particle Size in Ethylene Glycol. *ChemNanoMat* **2017**, *2*, 89-93.
- 200 7. Zemb, T.; Lindner, P., *Neutrons, X-rays and light: scattering methods applied to soft*
201 *condensed matter*. Elsevier: 2002.
- 202 8. Leontyev, I. N.; Kuriganova, A. B.; Leontyev, N. G.; Hennes, L.; Rakhmatullin, A.;
203 Smirnova, N. V.; Dmitriev, V., Size dependence of the lattice parameters of carbon supported
204 platinum nanoparticles: X-ray diffraction analysis and theoretical considerations. *Rsc Adv* **2014**,
205 *4* (68), 35959-35965.
- 206 9. Shi, C. Y.; Redmond, E. L.; Mazaheripour, A.; Juhas, P.; Fuller, T. F.; Billinge, S. J. L.,
207 Evidence for Anomalous Bond Softening and Disorder Below 2 nm Diameter in Carbon-
208 Supported Platinum Nanoparticles from the Temperature-Dependent Peak Width of the Atomic
209 Pair Distribution Function. *J. Phys. Chem. C* **2013**, *117* (14), 7226-7230.